Design and Development of Dual–Band Multi–Stage RF Energy Harvesting Circuit for Low Power Applications

Ankush Jolly, Mansi Peer, Vivek Ashok Bohara, Siddhant Verma
Wirocomm Research Group,
Department of Electronics and Communication,
IIIT-Delhi, India
Email: ankush12128@iiitd.ac.in, mansip@iiitd.ac.in, vivek.b@iiitd.ac.in, siddhant12165@iiitd.ac.in

***Abstract*—This paper presents the design and development of a dual–band multi–stage rectifier aimed at converting far field RF energy into DC voltage at low received power. The designed RF energy harvester consists of a dual–band matching network followed by a 3–stage rectifier which has been designed to work in GSM 900 MHz and Wi–Fi/Wireless LAN (WLAN) bands. It provides a peak conversion efficiency of 80% at 8 dBm received RF power at 915 MHz. The experimental results also show that the proposed dual–band rectifier can harness twice amount of power than single band 915 MHz rectifier. This work further utilizes the above circuit to obtain preliminary results of RF energy harvesting through mobile phones. Mobile phones from two different manufacturers have been used to evaluate the output DC voltage levels obtained through energy harvesting. Measurements were taken during call–establishment phase as well as during call–conversation phase. It was shown that depending on the manufacturer, it is possible to obtain peak average voltages of 1 volt and 0.25 volt in call–establishment phase and call–conversation phase respectively. The prototype has been fabricated on RT/Duroid 5880 substrate and all the simulations have been performed on Advanced Design System (ADS).**

***Keywords*—Output DC voltage, power conversion efficiency, rectifier, RF energy harvester.**

I. Introduction

Recently, significant amount of interest has been shown by the scientific research community into the domain of radio frequency (RF) energy harvesting as a means of "green" and non–polluting source of energy. The ubiquitous presence of ambient RF sources like cellular towers, mobile phones, Wi–Fi routers, television and radio transmitters in a humanized environment make the option of charging ultra–low power sensors by means of RF energy harvesting more feasible. RF energy unlike solar or wind [1] is more predictable as it is independent of the time of the day, weather/geographical location etc. and can be effectively provided on demand. Inductive coupling and magnetic resonance coupling are also other methods of wireless energy transfer (WET) which involve resonating of coils tuned at a particular frequency, however, there are two major limitations with this approach. First, the power is attenuated according to the cube of distance which restricts the power transfer distance. Second, it requires the calibration and alignment of resonators/coils which makes it difficult for mobile and remote charging [2].

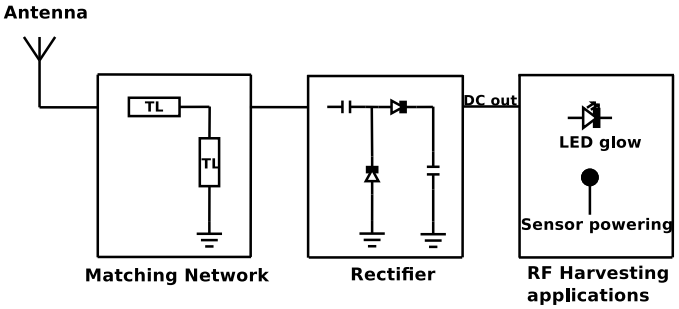

Fig. 1: Block diagram of an RF energy harvester

Wireless sensor networks (WSNs) have gained a considerable popularity nowadays due to their low cost and low power requirements. As a consequence, there is a large scale utilization of these sensor networks in many industrial and healthcare applications such as structural health monitoring, forest fire detection, pollution monitoring, logistics, security etc. [3],[4]. This evolution of wireless sensor networks has given birth to the notion of Internet of Things (IOT). However, deployment of large scale IOT devices is constrained by the dedicated source of energy required to operate these devices [5]. Furthermore, these devices are usually deployed in remote terrains or humanly inaccessible areas where replacing the source of energy is an arduous task. Thus, powering these sensors through RF energy would be a feasible option as suggested in [6], [7], [8].

A generic RF energy harvesting circuit, as shown in Fig. 1, consists of an antenna that captures the ambient RF signals, a matching network for maximum power transfer between antenna and rectifier, a rectifier that converts the incoming RF signal into DC voltage that can be further stored in a power management unit (PMU) or directly used for powering up the sensors. Most of the previous works on design and development of RF energy harvesting circuit have been based on single band harvesting including commercially available RF energy harvesters [9]. However, recent studies have shown that by harvesting energy from multiple and randomly distributed RF sources can lead to significant gains in the harvested power [10], [11], [12], [13]. In this paper, we have designed and developed a dual–band, 3–stage rectifier that converts the

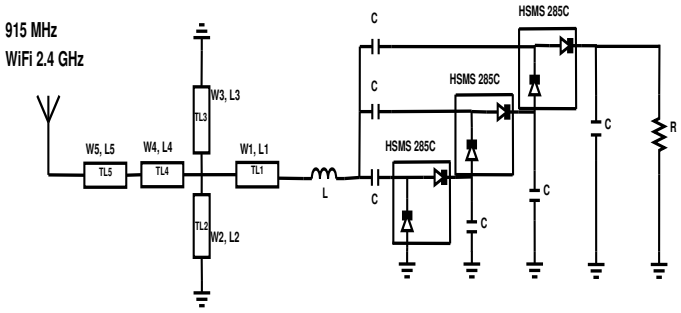

Fig. 2: Proposed dual–band rectifier with matching network

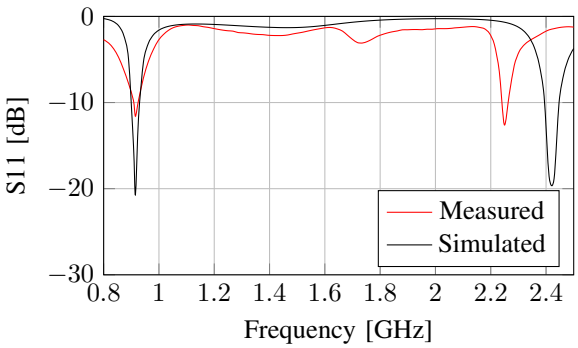

Fig. 3: Simulated and Measured S11 plot of EH rectifier

incident RF energy into DC power. The rectifier works at 915 MHz (GSM 900 MHz) and 2.4 GHz (Wi–Fi/WLAN band). The dual–band matching is based on multi stub matching as lumped element matching is not preferred for frequencies above 1 GHz. The circuit simulations have been done on ADS using Harmonic Balance (HB) simulation, which is a frequency domain circuit analysis technique for nonlinear circuits. This paper further investigates the energy harvesting ability of the rectifier from mobile phones operating in the GSM 900 MHz band. In order to validate the above, mobile phones of some well–known manufacturers such as Samsung and Motorola have been used. The energy harvesting capability of the designed RF energy harvesting circuit has been examined on the basis of its output DC voltage. The proposed work also highlights the fact that different mobile phones have different transmit power which impacts the efficiency and output DC voltage level of the energy harvesting (EH) circuit.

II. Rectifier Design

The rectifier is an important part of the RF energy scavenger as a proper design of rectifier can significantly enhance the RF to DC conversion efficiency. Power conversion efficiency (PCE) is the most important parameter to analyse the performance of the rectifier circuit. As shown in (1), P_{in} is the incident RF power while P_{DC} is the output DC power and η defines how much incident RF power has been converted into DC power.

$$\eta = (P_{DC}/P_{in}) \times 100 \quad (1)$$

A. Diode Specifications

To achieve high efficiency of RF–to–DC conversion at low RF power, schottky diodes are preferred over normal diodes as they have faster switching speed, low diode losses due to their metal–semiconductor junction and a forward voltage drop of 150 mV. In our proposed design, the schottky diode HSMS 285C from Avago Technologies was selected.

B. Rectifier Circuit

As shown in Fig. 2, we have implemented a 3–stage rectifier circuit which acts as a voltage multiplier. Though increasing the number of stages increases the rectified voltage at the output, but it results in longer charging time of the capacitors due to the increase in stray capacitance and reduction in current across the load resistor. Moreover, it also results in higher ripples in the output voltage. Hence, to obtain an optimum balance of DC output voltage and current, a rectifier with three stages was designed in ADS. The rectifier circuit has been terminated with a 10 kΩ resistor.

C. Matching Network

The matching network plays a crucial role in power transfer between the antenna and rectifier. We have implemented a dual–frequency matching scheme [14] capable of simultaneously matching frequency dependent complex loads (FDCLs) having different values at frequencies of interest i.e. 915 MHz and 2.42 GHz to a real source impedance of 50 Ω. Fig. 3 depicts the simulation and measured results of the input return loss. Due to imprecise manual soldering and higher parasitic impedance of Schottky diode at high frequencies, the desired matching at 2.42 GHz has been shifted to 2.25 GHz while it is matched at 915 MHz. For improved matching, resistance compression network (RCN) can be used [15]. RCN minimizes the sensitivity of the rectifier to changing input power and load conditions. Hence, smaller variations in input impedance of the rectifier can lead to a better performance.

III. Experimental Results

A. Rectifier Efficiency Measurement

The fabricated prototype of the proposed rectifier is shown in Fig. 4(a). It has been fabricated using Rogers RT/Duroid 5880 substrate with a dielectric constant, $\epsilon_r \approx 2.2$ and a dissipation factor $\tan\delta \approx 0.0009$. The total size of the prototype is about 15 cm X 10 cm. The rectifier is terminated with a 10 kΩ resistor to measure DC voltage and power. Due to imperfect soldering, the load resistance value was measured to be 8.2 kΩ Fig. 4(b) exhibits the setup used for calculating the rectifier efficiency and output voltage.

Since there is a mismatch at 2.42 GHz, all the measurements were taken at 2.25 GHz. This designed RF energy harvesting circuit was evaluated by feeding with direct RF power from the signal generator. Fig. 5 and Fig. 6 show the simulated and measured efficiency and output DC voltage of the rectifier at 915 MHz and 2.25 GHz respectively. As it can be observed from the plot, the maximum measured efficiency at 915 MHz is 80% at 8 dBm input RF power while it is 30% at 2.25 GHz.

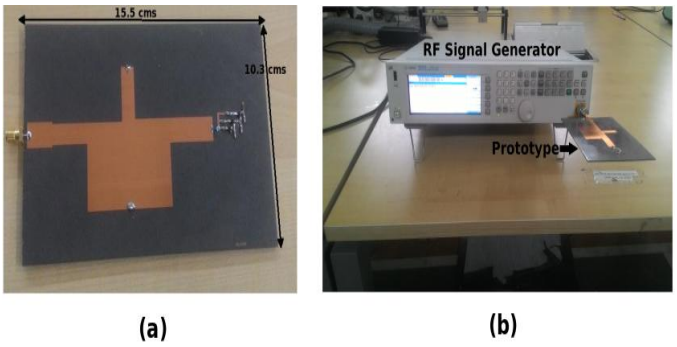

Fig. 4: (a) Fabricated prototype (b) Prototype connected with RF signal generator

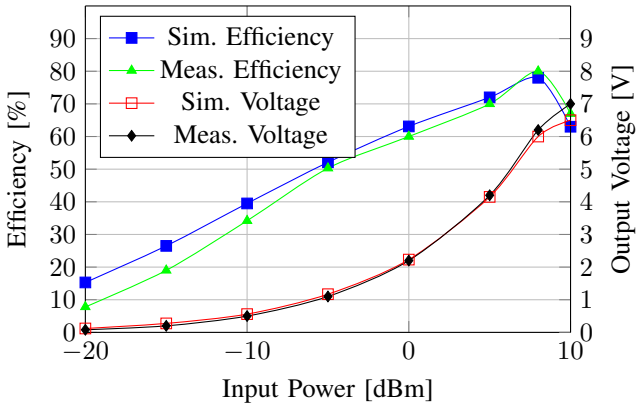

Fig. 5: Simulated and Measured Results at 915 MHz

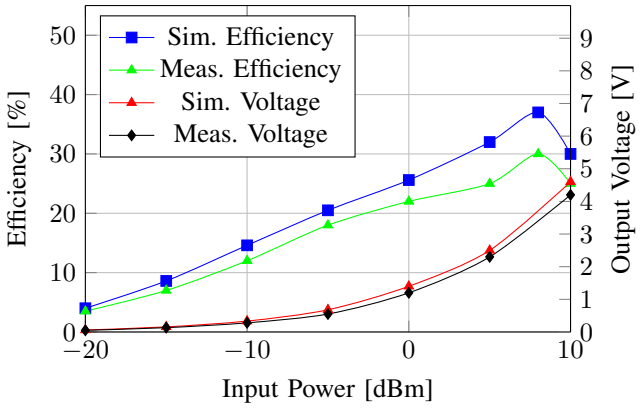

Fig. 6: Simulated and Measured Results at 2.25 GHz

B. Dual–band RF harvesting measurement

Fig. 7 exhibits the setup to measure the output DC voltage and harvested power. R&S®HF907 [16] horn antenna with a gain of up to 14 dBi has been used as a receiving antenna for the RF energy harvesting circuit. This antenna has high directivity in the frequency range of interest. The measurement setup was conducted in an indoor environment (inside an anechoic/insulated chamber). An RF signal generator was used to generate 10 mW power at 915 MHz and 2.25 GHz and kept at a distance of 1m and 0.5m respectively from the receiver.

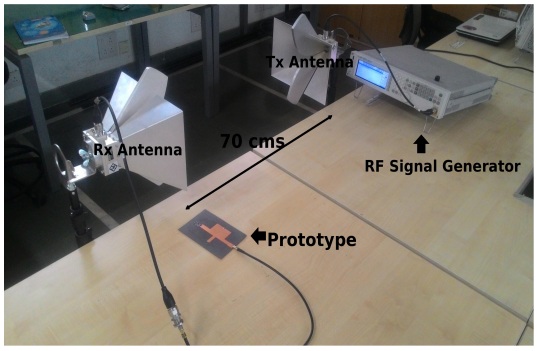

Fig. 7: Dual–band EH measurement

The receiver side was connected with the fabricated prototype. The measurement results are shown in Table I. Dual–band harvesting harnesses 0.088 mW which is twice of the power harvested at 915 MHz i.e. 0.043 mW and 1.8 times more than the individual bands (915 MHz and 2.25 GHz) combined. The amount of power generated (88 μW) is enough to power sensors which are used for IOT applications as shown in Table II. Table III shows the performance comparison of our work with the existing work on dual–band RF harvesting on parameters like maximum efficiency achieved, received RF power range for which PCE is greater than 30% and minimum received RF power required to generate output DC voltage of 1V.

TABLE I: Dual–band Measured Results

Source 1 Freq: 915 MHz Distance: 1m	Source 2 Freq: 2.25 GHz Distance: 0.5m	Output DC Voltage (V)	DC Power (mW)
ON	OFF	0.6	0.043
OFF	**ON**	0.24	0.007
ON	**ON**	0.85	0.088

C. Energy Harvesting Measurement from Smartphones

In the following, we utilize the circuit developed to obtain preliminary results of RF energy harvesting through mobile phones [22]. To explore the feasibility of the above, we measured the RF power emitted by the mobile phones using spectrum analyzer when the mobile is operating in uplink and is placed near to the receiving antenna. The measured Received Signal Strength Indicator (RSSI) has been demonstrated through the spectrum plot in Fig. 8. It can be observed from Fig. 8 that there is a spike in RF power level when a call is initiated by the mobile phone. It was also observed that the RSSI from mobile phones usually fluctuate depending

TABLE II: Power Consumption level of sensors

Sensor Application	Power Consumption (μW)
Temperature Sensor [17]	10
Humidity Sensor [18]	10.32
Sensor for Bicycle Torque performance measurements [19]	17
Wake-up receiver for Wireless Sensor Networks (WSNs) [20]	6.8
RFID-based sensor [21]	7

TABLE III: Performance Comparison

Design	Our Work	[10]	[11]	[12]	[13]
Technology	Schottky Diode (HSMS 285C)	Schottky Diode (SMS 7630)	Schottky Diode (HSMS 285C)	Schottky Diode (HSMS 285C)	Schottky Diode (HSMS 286x)
Band	Dual-band	Dual-band	Dual-band	Triple-band	Dual-band
Frequency (GHz)	0.915/2.25	0.915/2.45	2.1/2.45	0.94/1.95/2.44	0.92/2.4
Matching Network	Multi-stub	RCN	Multi-stub	LC Boost network	LC Boost Network
Efficiency	80% @ 915 MHz, 8 dBm 30% @2.25 GHz, 8 dBm	42% @ 915 MHz, 0 dBm 38% @ 2.45 GHz, 0 dBm	24% @ 2.1 GHz, 10 dBm 18% @ 2.45 GHz, 10 dBm	80% @ 940,MHz, 10 dBm 42% @ 2.44 GHz, 16 dBm	78% @ 920 MHz, 15 dBm 70% @ 2.4 GHz, 15 dBm
Pin (dBm) range for eff. >30%	-12 to 20	>-10 to 0	NA	-9 to 20	-3 to 20
Pin (dBm) for output vol. >1V	-6 dBm @ 915 MHz -1 dBm @ 2.25 GHz	NA	4 dBm @ 2.1 GHz 5 dBm @ 2.45 GHz	NA	1 dBm @ 920 MHz 5 dBm @ 2.4 GHz

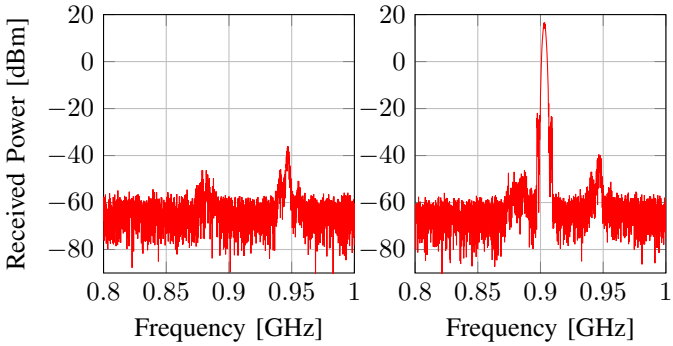

Fig. 8: Spectrum Plots (a) No call (b) During call at one time instant

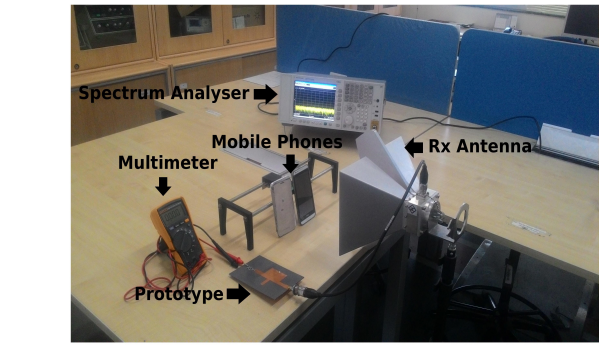

Fig. 9: EH measurement from smartphones

on the channel conditions, distance from cellular towers, etc. Two smartphones, from popular manufacturers, namely Galaxy Grand Max from Samsung and Moto X from Motorola have been used for the experiment. Since mobile handsets can transmit up to 2 Watts depending on channel conditions and distance from cell towers, the idea of harvesting RF power from mobile phones can revolutionize future mobile handsets.

Fig. 9 exhibits the setup used for measuring output DC voltage from a mobile phone. The measurements were recorded while keeping the mobile phones in close proximity of the EH circuit. For experimental validation of the proposed setup,

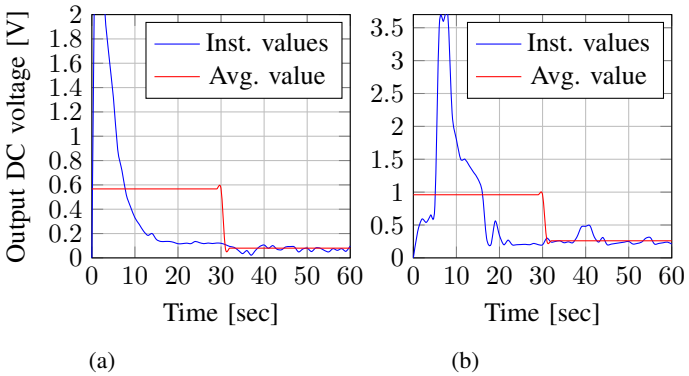

(a) (b)

Fig. 10: (a) Moto X Measurements (b) Samsung Galaxy Grand Max Measurements.

handsets were deliberately chosen to operate in 2G mode so that calls are made in GSM 900 MHz band. The data was collected over multiple calls from each handset. The total call duration was 1 minute which was divided into two parts : 30 seconds of call–establishment phase (it includes, connection time, ringing time) and 30 seconds of call–conversation phase. The average DC voltage of the calling sessions has been plotted for each handset. Apart from the instantaneous values, an average DC voltage corresponding to the first 30 seconds and an average corresponding to last 30 seconds has also been plotted to demonstrate the difference in RF power levels between the two phases. Fig. 10 (a) and 10 (b) show the output DC voltage for Moto X and Galaxy Grand Max respectively. The average DC voltage for first thirty seconds for Grand Max and Moto X is 1 V and 0.58 V respectively and for the next thirty seconds, it is 0.25 V and 0.1 V respectively. One more observation from Fig. 10 (a) and Fig. 10 (b) is that the output DC voltage has dropped by 13.5 dB (average of both plots) between call–establishment phase and call–conversation phase. We also observed that during the call–conversation phase, output voltage is on a higher side when voice activity is higher as compared to low periods of voice activity. The average DC voltage obtained over the two call phases for Galaxy Grand Max smartphone can be easily found to be

$$\text{Average DC voltage} = \frac{1\text{ V} + 0.25\text{ V}}{2} = 0.625\text{ V}. \quad (2)$$

Hence, the amount of power harvested can be calculated as

$$\text{Power harvested} = \frac{V^2}{R} = (0.625\ \text{V})^2/(8.2\ \text{k}\Omega) = 0.047\ \text{mW}. \quad (3)$$

As mentioned earlier in Table II, the amount of power harvested is enough to operate low power sensors. This type of circuit can be installed in public places like train stations, malls, etc. where there are many people around who are using mobile phones. Moreover, this study can be further investigated and more amount of power can be harvested if the circuit also operates in Wi–Fi band as time spent by consumers on mobile data usage is much more than the time spent in making calls. Energy harvesting from mobile phones is still in nascent stage. These results support the claim that smartphones can be used to harness energy, provided that the circuit can be made sensitive enough to harness power at even lower received power (< -30 dBm) which is the subject of future work.

IV. Conclusion

This paper presented the design of a dual–band multi–stage rectifier along with the matching technique based on multi–stub matching. In order to operate the rectifier at low input power and high frequency, schottky diode HSMS 285C was used. The proposed design provides maximum efficiency of 80% and an output voltage of 6V at 915 MHz with 8 dBm input RF power. At 2.25 GHz, maximum efficiency of 30% and output voltage of 3V was achieved. It was also shown that simultaneous dual–band RF harvesting provides better efficiency and harvested power than single band RF energy harvesting. This work also presented some preliminary results on harvesting energy from smartphones in GSM 900 MHz band. This harvested energy can be used to power low power wireless sensor nodes. The proposed work can be further extended to harvest energy from the Wi–Fi/WLAN band and this will be the subject of future work.

References

[1] G. H. Millard, "Wind- and sun-powered transmitters," *IEEE Proceedings A - Physical Science, Measurement and Instrumentation, Management and Education - Reviews*, 1982.

[2] X. Lu, P. Wang, D. Niyato, D. I. Kim, and Z. Han, "Wireless networks with rf energy harvesting: A contemporary survey," *IEEE Communications Surveys Tutorials*, vol. 17, no. 2, pp. 757–789, Secondquarter 2015.

[3] A. Pantelopoulos and N. G. Bourbakis, "A survey on wearable sensor-based systems for health monitoring and prognosis," *IEEE Transactions on Systems, Man, and Cybernetics, Part C (Applications and Reviews)*, vol. 40, no. 1, pp. 1–12, Jan 2010.

[4] V. C. Gungor and G. P. Hancke, "Industrial wireless sensor networks: Challenges, design principles, and technical approaches," *IEEE Transactions on Industrial Electronics*, vol. 56, no. 10, pp. 4258–4265, Oct 2009.

[5] C. Alippi, G. Anastasi, M. D. Francesco, and M. Roveri, "Energy management in wireless sensor networks with energy-hungry sensors," *IEEE Instrumentation Measurement Magazine*, vol. 12, no. 2, pp. 16–23, April 2009.

[6] T. B. Lim, N. M. Lee, and B. K. Poh, "Feasibility study on ambient rf energy harvesting for wireless sensor network," in *Microwave Workshop Series on RF and Wireless Technologies for Biomedical and Healthcare Applications (IMWS-BIO), 2013 IEEE MTT-S International*, Dec 2013, pp. 1–3.

[7] M. Peer, N. Jain, and V. A. Bohara, "A hybrid spectrum sharing protocol for energy harvesting wireless sensor nodes," in *2016 IEEE 17th International Workshop on Signal Processing Advances in Wireless Communications (SPAWC)*, July 2016, pp. 1–6.

[8] T. Kalluri and V. A. Bohara, "Regenerative relaying in energy harvesting cognitive radio networks," in *2016 European Conference on Networks and Communications (EuCNC)*, June 2016, pp. 84–88.

[9] P2110 lifetime power® energy harvesting development kit for wireless sensors. [Online]. Available: http://www.powercastco.com/products/development-kits

[10] K. Niotaki, A. Georgiadis, A. Collado, and J. S. Vardakas, "Dual-band resistance compression networks for improved rectifier performance," *IEEE Transactions on Microwave Theory and Techniques*, vol. 62, no. 12, pp. 3512–3521, Dec 2014.

[11] E. Khansalee, Y. Zhao, E. Leelarasmee, and K. Nuanyai, "A dual-band rectifier for rf energy harvesting systems," in *2014 11th International Conference on Electrical Engineering/Electronics, Computer, Telecommunications and Information Technology (ECTI-CON)*, May 2014, pp. 1–4.

[12] B. L. Pham and A.-V. Pham, "Triple bands antenna and high efficiency rectifier design for rf energy harvesting at 900, 1900 and 2400 mhz," in *Microwave Symposium Digest (IMS), 2013 IEEE MTT-S International*, June 2013, pp. 1–3.

[13] Q. Zhao, J. Xu, H. Yin, Z. Lu, L. Yue, Y. Gong, Y. Wei, and W. Wang, "Dual-band antenna and high efficiency rectifier for rf energy harvesting system," in *2015 IEEE 6th International Symposium on Microwave, Antenna, Propagation, and EMC Technologies (MAPE)*, Oct 2015, pp. 682–685.

[14] M. S. H. M. A. Maktoomi and V. Panwar, "A dual-frequency matching network for fdcls using dual-band λ/4-lines," *Progress In Electromagnetics Research Letters*, vol. 52, no. 2, pp. 23–30, 2015. [Online]. Available: http://www.jpier.org/PIERL/pier.php?paper=15020405

[15] Y. Han, O. Leitermann, D. A. Jackson, J. M. Rivas, and D. J. Perreault, "Resistance compression networks for radio-frequency power conversion," *IEEE Transactions on Power Electronics*, vol. 22, no. 1, pp. 41–53, Jan 2007.

[16] R&s®hf907 antenna. [Online]. Available: https://www.rohde-schwarz.com/in/product/hf907-productstartpage_63493-7982.html

[17] P. Chen, C.-C. Chen, C.-C. Tsai, and W.-F. Lu, "A time-to-digital-converter-based cmos smart temperature sensor," *IEEE Journal of Solid-State Circuits*, vol. 40, no. 8, pp. 1642–1648, Aug 2005.

[18] Z. Tan, R. Daamen, A. Humbert, Y. V. Ponomarev, Y. Chae, and M. A. P. Pertijs, "A 1.2-v 8.3-nj cmos humidity sensor for rfid applications," *IEEE Journal of Solid-State Circuits*, vol. 48, no. 10, pp. 2469–2477, Oct 2013.

[19] S. K. Gharghan, R. Nordin, and M. Ismail, "An ultra-low power wireless sensor network for bicycle torque performance measurements," *Sensors*, vol. 15, no. 5, May 2015.

[20] K. Takahagi, H. Matsushita, T. Iida, M. Ikebe, Y. Amemiya, and E. Sano, "Low-power wake-up receiver with subthreshold cmos circuits for wireless sensor networks," *Analog Integrated Circuits and Signal Processing*, vol. 75, no. 2, pp. 199–205, 2013. [Online]. Available: http://dx.doi.org/10.1007/s10470-012-9929-1

[21] N. Gay and W. J. Fischer, "Ultra-low-power rfid-based sensor mote," in *2010 IEEE Sensors*, Nov 2010, pp. 1293–1298.

[22] A. Jolly, M. Peer, and V. A. Bohara, "Powering future mobile phones through RF energy harvesting," *CoRR*, vol. abs/1702.03799, 2017. [Online]. Available: http://arxiv.org/abs/1702.03799